A semisynthetic peptide-metalloporphyrin responsive matrix for artificial photosynthesis

Sun, Z.

Chapter 6

General discussion and outlook

6.1 Structure assessment

Advances in the constitution of the self-assembly of a semi-synthetic zinc-protoporphyrin IX (ZnPP) peptide (tCsmA) complex derived from the natural CsmA light harvesting antenna has led to more insight in the responsive chiral matrix in the photosystems. The tCsmA-ZnPP complex is able to self-assemble to form extended periodic 7_2 helical filaments after dialysis in KPi buffer (Chapter 2 and Chapter 4). The 7_2 helical structure of the self-assembled tCsmA-ZnPP complex is resolved at about 7 Å resolution by the cryo-EM technique. The tCsmA peptide, which contains 43 amino acids, is derived from the CsmA scaffolding peptide in the baseplate of *C. tepidum* by removing the flexible segments from the N and C-termini. The tCsmA successfully maintains the functional central α-helix (Chapter 3). The ZnPP coordinate to the only histidine of tCsmA. For the tCsmA-ZnPP complex in KPi buffer, each strand prefers to twist to form a stable helical structure. As a result, the hydrophobic side of the tCsma-ZnPP structural motif in the helical fibrils are rotated nearly 90° compared to the CsmA in the planar baseplate in the natural system. The tCsmA forms a hydrophobic core which leads the ZnPP to locate at the inside of the peptide scaffold. The charged residues are exposed towards the outside and can form salt bridges with other filaments to form bundles, which was shown in Chapter 3.

The electron density map for the monomeric building block shows continuous density of protein, which indicates an extended alpha helical structure without any loop regions. Therefore the loop from residue 30 to residue 35 that was observed in NMR data collected from CsmA in solution probably transforms to an extended helical structure for the tCsmA-ZnPP complex self-assembly. Each strand in the 7_2 helix is composed of dimeric tCsmA-ZnPP complexes in an antiparallel arrangement with P2 symmetry. The two ZnPP in each dimeric unit are close to the neighbouring ZnPP from a building block in the other strand and form a stable tetrameric unit.

Different from the baseplate structure, for the 7_2 helix salt bridges are of little importance for the self-assembly. The packing strongly suggests that dipole-dipole interactions involving ZnPP may play a role in the self-assembly.

The electron density map also shows a small bump around the ZnPP, which can be one of the propionic acid groups -CH_2-CH_2-COOH (Chapter 4). A rigid density indicates that the propionic acid group may interact with the peptide and is fixed by *e.g.* a hydrogen bond interaction. The tCsmA-ZnPP complex shows some similarity with the natural CsmA-BChl *a* complex. The distance between the ZnPP in the dimeric units also is about 21.1 Å. Moreover, two complexes cross with a similar angle as for the natural system.[1]

Although Tris buffer cannot be used as the dialysis buffer for the complex constitution, the complex obtained in KPi buffer remains intact when it is dialyzed against Tris buffer. During the buffer change, most filaments turn into smaller pieces without degradation. However, part of the structure of helix transforms to a planar structure, which resembles the natural CsmA baseplate antenna. The distance between strands is found to be same as for the natural baseplate, which is about 31.3 Å. The ZnPP are also embedded in the middle of the strands. Their macrocycles are oriented perpendicular to the plane of the assembly. We attribute these planar structures to untwisting of helical filaments upon changing the buffer. While in the helix the ZnPP interact to form a tetramer, in the planar form the ZnPP form extended linear arrays of dimeric ZnPP in between two tCsmA strands (Chapter 3). The optical data indicate that the ZnPP may be less planar in Tris buffer relative to KPi buffer. Although the packings of the two types of self-assembly are different, planar versus helical, their CD responses strongly overlap (Chapter 3). That indicates that overall the tCsmA helical peptide undergoes little conformational change of the secondary structure on the peptide level upon buffer change.

6.2 Constitution

We tested different truncated CsmA homologues for the constitution with ZnPP. However, only tCsmA prepared by N-terminal acetylation and C-terminal amidation to replace the flexible segments in the natural peptide is able to bind with ZnPP and form a large self-assembly. It is probably the

net charge of the peptides that influences the constitution (Chapter 3). Because the basic nitrogen atom in the imidazole of histidine with a lone electron pair can coordinate to metallic cations like the Zn^{2+} of ZnPP when pH>7. The binding is efficient at higher pH of the dialysis buffer, up to pH 7.9.

The molar extinction coefficient of the ZnPP in complex with tCsmA is 117400 M^{-1} cm^{-1} with a stoichiometry of tCsmA : ZnPP ~ 1 : 1 (Chapter 2). The constitution can be done in 1-propanol KPi buffer or in KPi buffer containing detergents with high CMC such as HG or OG detergents. Compared to the 1-propanol KPi buffer, the detergents buffers lead to a slow dialysis process but higher binding efficiency (Chapter 3).

6.3 Photochemical relevance

The photo-degradation occurs during a prolonged light exposure. The complex can be dissociated when it is exposed to sunlight for a few hours. The reason for the photo-dissociation might be that the dissipation of heat is slow. However, despite photo-dissociation on longer time scales, the tCsmA-ZnPP complex is able to maintain a short time photostability. It occurs when a high concentration more than 20 µM of the complex is excited by 430 nm UV light. Recently, it has been proposed that light-driven conformational changes in chiral protein scaffolds can develop vibronic states within or between linear arrays. It may suggest that distribution of energy helps to dissipate the excess energy and may be of vital importance for further improvement of the stability (Chapter 2).

In Chapter 2, the tCsmA-ZnPP complex shows 594 nm and 650 nm emission peaks after excitation. The MV^+ has a strong broad absorption at 606 nm (ε = 13700 M^{-1} cm^{-1}). When the acceptor cation radical methyl viologen (MV^+) was added in the complex solution, the harvested light from the tCsmA-ZnPP complex can be 100% quenched by MV^+. This leads us to conclude that intermolecular FRET or Dexter energy transfer between ZnPP and MV^+ may cause fluorescence quenching by energy transfer due to overlapping spectra. On the other hand, the quenching is dependent on the concentration of MV^+. When the concentration was increased to about 300 µM MV^+ in the tCsmA-ZnPP solution, nearly all fluorescence of ZnPP was quenched.

The fluorescence decay responses of the tCsmA-ZnPP complex at 594 nm and 650 nm can be described with 3 different lifetime components. It is found that all three lifetimes of the complex with the MV^+ additive are shortened, especially τ_3 was dramatically shortened to ~1 ps and the energy is almost 100% quenched by the acceptor. This is comparable to natural light-harvesting antenna systems (Chapter 2).

The MV^+ in solution was obtained with the help of sodium dithionite. The sodium dithionite is able to offer one electron to MV^{2+} to form MV^+. When sodium dithionite is depleted by letting it react with oxygen, the MV^+ is converted back to MV^{2+}. When MV^+ is oxidized to MV^{2+}, it shows no fluorescence quenching any more. Moreover, the quenched complex recovered the same fluorescence as without acceptor. It indicates that the complex still maintains its integrity upon photoexcitation (Chapter 2). This highlights the importance of the MV^+ as the quenching species.

6.4 Future experiments

6.4.1 Functional exploration

In Chapter 2, the tCsmA-ZnPP complex shows the ability of light-harvesting and energy transfer. Further experiments can be done to explore how to increase the stability of the complex, and to improve the efficiency and mechanism of energy transfer. This will be helpful for the design of semisynthetic systems for light harvesting and their application in solar fuel cells. The Cyclic Voltammetry (CV) measures the current that develops in an electrochemical cell under conditions where voltage is in excess of that predicted by the Nernst equation.[2-4] Therefore CV experiments are able to observe the electron transfer to check the functional relevance of the tCsmA-ZnPP complex for charge transfer.[5-6] For the further application, it is also interesting to attach the tCsmA-ZnPP complex to an electrode and build a prototypic solar cell device, as schematically depicted in Figure 6.1.

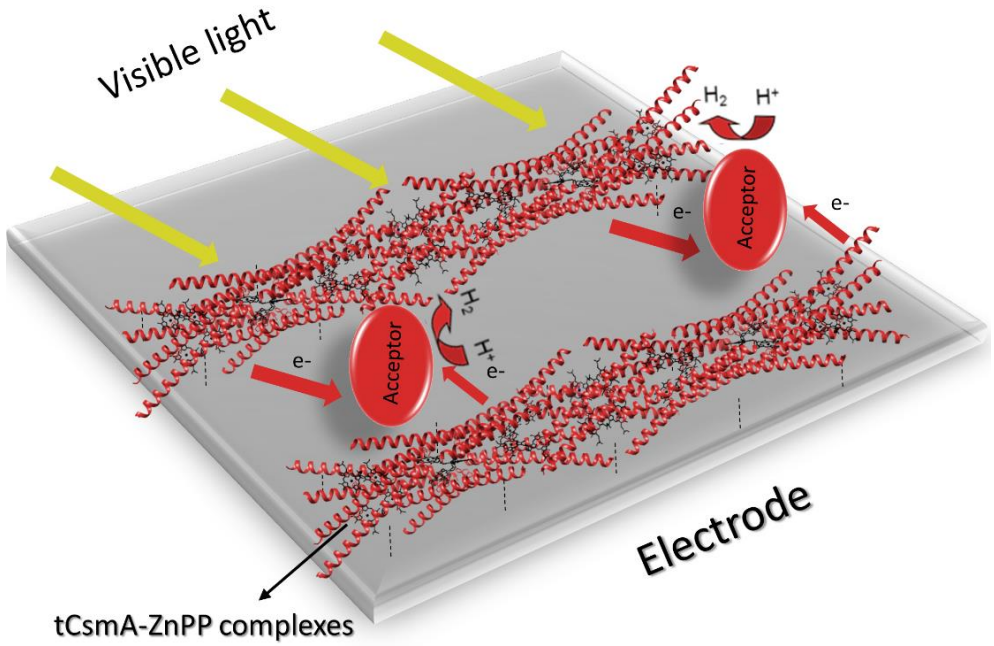

Figure 6.1 Schematic design of a solar cell device. The tCsmA-ZnPP complex could be modified to attach to the electrode surface.

6.4.2 Atomic structure determination

Despite good progress, atomic information was not yet obtained. There are two methods, NMR and cryo-EM, that can be used for resolving structure at high resolution. For NMR, some sample preparation work has been done in Chapter 5. It shows that without a large fusion tag, tCsmA rapidly degrades. In addition, TRX and MBP tags are used to get protein. However, with TRX the stability can be increased, but the sample precipitates making further treatment difficult. With the MBP tag a strongly associated soluble tCsmA-MBP construct is obtained, but only little protein can be purified. Thus, to continue the further experiments, more tags should be tried. Since preliminary data have shown that the peptides are expressed in vitro and can be purified without degradation, this may be the best route to follow for further optimization. Before the purification of recombinant variants of truncated CsmA, the sequence should be modified and optimized for constitution. As the data in Chapter 3 shows, the net charge of the protein influences the binding. The truncated CsmA are derived from the natural

CsmA by cutting off the flexible segments. The net charge is changed by the truncation. Therefore the sequence should be optimized first.

For cryo-EM, the low resolution is caused by a thick ice layer. This results in a high scattering mass and more noise in comparison to thin layer samples.[7] Hence the sample preparation process can be optimized for better resolution. In particular, the sample can be improved to obtain a thinner ice layer with a longer blotting time or by adjusting the humidity during the blotting. During the image collection, a higher dose of electrons can be tried to get more contrast.

6.5 References

1. Nielsen, J. T.; Kulminskaya, N. V.; Bjerring, M.; Linnanto, J. M.; Rätsep, M.; Pedersen, M. Ø.; Lambrev, P. H.; Dorogi, M.; Garab, G.; Thomsen, K., *Nature communications* **2016,** *7*, 12454.
2. Nicholson, R. S.; Shain, I., *Analytical Chemistry* **1964,** *36* (4), 706-723.
3. Heinze, J., *Angewandte Chemie International Edition in English* **1984,** *23* (11), 831-847.
4. Elgrishi, N.; Rountree, K. J.; McCarthy, B. D.; Rountree, E. S.; Eisenhart, T. T.; Dempsey, J. L., *Journal of Chemical Education* **2018,** *95* (2), 197-206.
5. Li, Q.; Luo, G.; Feng, J., *Electroanalysis* **2001,** *13* (5), 359-363.
6. Hirst, J.; Armstrong, F. A., *Analytical Chemistry* **1998,** *70* (23), 5062-5071.
7. Wu, S.; Armache, J.-P.; Cheng, Y., *Microscopy (Oxf)* **2016,** *65* (1), 35-41.